

# Inverse Design in the Complex Plane: Manipulating Quasi-Normal Modes

J. R. Capers,<sup>1,\*</sup> D. A. Patient,<sup>1,†</sup> and S. A. R. Horsley<sup>1</sup>

<sup>1</sup>*Department of Physics and Astronomy,  
University of Exeter, Stocker Road, Exeter, EX4 4QL*

(Dated: June 29, 2022)

## Abstract

Utilising the fact that the frequency response of a material can be decomposed into the quasi-normal modes supported by the system, we present two methods to directly manipulate the complex frequencies of quasi-normal modes in the complex plane. We first consider an ‘eigen-permittivity’ approach that allows one to find how to shift the permittivity of the structure everywhere in order to place a single quasi-normal mode at a desired complex frequency. Secondly, we then use perturbation theory for quasi-normal modes to iteratively change the structure until a given selection of quasi-normal modes occur at desired complex frequencies.

---

\* jrc232@exeter.ac.uk

† dp348@exeter.ac.uk

## I. INTRODUCTION

Quasi-normal modes (QNMs) are the complex frequency bound states of a system. They were first used in quantum mechanics to describe alpha decay [1, 2], and have since found utility in modelling radiation in many different systems, from black holes [3] to photonic resonators [4]. QNMs correspond to the poles of the scattering matrix in the complex frequency plane [5, 6], where the waves at the boundary of the system are purely outgoing. The effect of a structured environment can, for example, be analysed by decomposing the Purcell factor in terms of these QNMs [7], and through calculating how small changes in the system perturb the QNMs, deeper insight into sensing has been developed [8, 9]. Here, motivated by the connection between the location of poles in the complex plane and physical properties such as transmission, we combine ideas from inverse design with the QNM approach to modelling resonator systems to design materials which have poles at specific complex frequencies.

Perhaps the simplest example of a system supporting QNMs is a homogeneous dielectric slab (refractive index  $n_R$  in some background index  $n_B$ ). For this simple case, the complex frequencies of the QNMs can be found analytically [3, 4] as

$$k_m L = \frac{2\pi m + i \ln [(n_R - n_B)^2 / (n_R + n_B)^2]}{2n_R}, \quad (1)$$

where  $m$  is an integer and  $L$  is the width of the slab. Figs. 1(a-c) demonstrate that poles in the reflectivity as a function of complex  $k$  correspond to QNMs, which are in turn associated with peaks in transmission. Examining the field, shown in Fig. 1(c), at a complex  $k$  value associated with a QNM shows the characteristic exponential growth in space.

More complicated systems can also be understood in terms of QNMs. One example is the absorbing stack designed numerically, and experimentally verified by Sakurai et al. [10]. Consisting of alternating layers of dielectric on a metal substrate, the device performs as a near perfect absorber in the mid-infrared. The absorption of this structure, along with the reflectivity in the complex wavelength plane is shown in Figs. 1(d-e). Fitting the Lorentzian

$$\mathcal{L}(\lambda) = \frac{\Gamma}{(\lambda - \lambda_0)^2 + \Gamma^2} \quad (2)$$

to the absorption peak, we find the peak wavelength is  $\lambda_0 = 5.15\mu\text{m}$  and the linewidth  $\Gamma = 0.0138\mu\text{m}$ . This corresponds to a pole of the reflection coefficient in the complex plane at  $\lambda_0 + i\Gamma$ , as shown in Fig. 1(e).

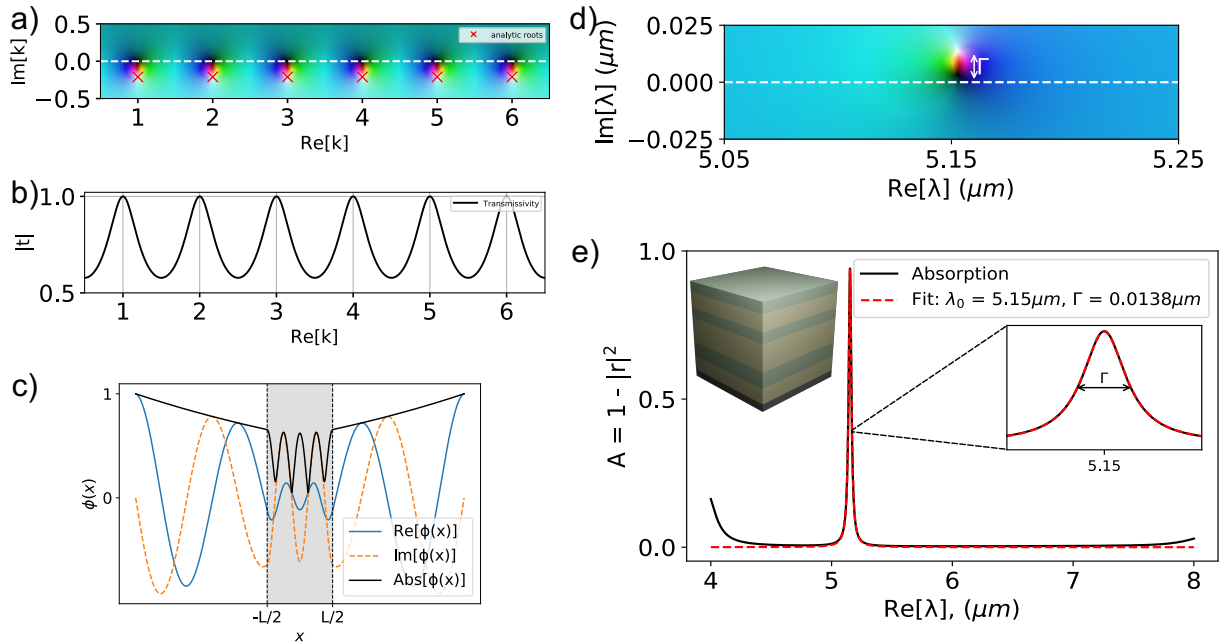


FIG. 1: The quasi-normal modes of a dielectric slab (a-c) and the absorbing stack (d-e). The reflection in the complex plane (a) and transmission  $(1 - |r|^2)$  along the real frequency axis (b). The red crosses represent the analytic solution to Eq. (1) for  $n_b = 1$ ,  $n_r = \pi$ ,  $L = 1$ . The real component of the QNMs are associated with the peaks in transmission. The real (blue), imaginary (orange dashed) and absolute (black) field distribution (c) of the  $m = 3$  mode is shown to have the characteristic exponential growth in space. For the (near) perfect absorber (depicted in inset, green layers are Germanium, yellow are Silicon Oxide, with a Tungsten substrate), the complex reflectivity (d) shows a single QNM. The absorption spectrum (e) shows a large resonance in the mid-IR, with a resonant frequency ( $\lambda_0$ ) and linewidth ( $\Gamma$ ) directly associated with the QNM, as demonstrated by the fitting of a Lorentzian to the absorption spectra (red dashed line).

While QNMs provide a valuable framework to understand resonators, the ability to *design* the spectral response of materials is key to more efficient photovoltaic cells [11] and sensors [12]. For sensing applications, narrow resonances at particular wavelengths are desirable [13–15], while energy harvesting requires large absorption over a broad band [16–19].

Designing electromagnetic materials for specific applications has attracted much recent attention [20]. When designing spectral features, one can employ the physical insight provided by QNMs to greatly simplify the problem. For example, one way to approach the

inverse design problem for absorbers is to try to move the QNM to a desired complex frequency [21]. In this way, one can tailor scattering effects [22], design absorbers [23] and manipulate exceptional points [24] with minimal numerical complexity. To date, however, these approaches address the forwards problem, finding how the pole moves if the resonator geometry is changed. We instead solve the inverse design problem of designing materials with poles at specific complex frequencies, using only simple techniques. Throughout this work, results are obtained by either back-integrating the Helmholtz equation using Scipy’s ‘odeint’ [25], or using the transfer matrix [26], although comparisons with full-wave solutions in COMSOL Multiphysics [27] are provided.

We present two methods for placing QNM poles at arbitrary complex frequencies. Firstly, we re-formulate the eigenvalue problem of the Helmholtz equation to find a complex constant value by which the permittivity of a structure should be shifted to place a pole in the desired location. Secondly, we employ QNM perturbation theory to find how to change the spatial distribution of material to move around several poles in the complex frequency plane. These methods enable the simultaneous control of resonance wavelength *and* linewidth, for the design of absorbers and sensors.

## II. EIGEN-PERMITTIVITIES

One way to *find* the locations of quasi-normal modes (QNMs) is to formulate the Helmholtz equation for the out-of-plane electric field  $\phi$ , as an eigenvalue problem for complex wave-numbers  $k$

$$-\frac{1}{\varepsilon(x)} \frac{d^2\phi}{dx^2} = k^2\phi. \quad (3)$$

However, to find the QNMs the correct boundary condition must be imposed on  $\phi$ . Originally derived by Sommerfeld [28], but since used to model black hole radiation [29, 30], the appropriate boundary condition is that the wave is purely outgoing. For example, on the right hand side of a planar medium,

$$\frac{d\phi(x)}{dx} = ik\phi(x), \quad (4)$$

as  $x \rightarrow +\infty$ . To numerically find the QNMs of our system, we imposed this boundary condition within a finite difference approximation, adapting the elements of the Laplacian at the boundaries (e.g. for  $N$  points the value of the field at the final point on the right of

the system is fixed to be  $\phi_{N+1} = \phi_N + ik\Delta x\phi_N$ , giving

$$\frac{d^2\phi}{dx^2} \approx \frac{1}{(\Delta x)^2} \begin{pmatrix} (ik\Delta x - 1) & 1 & 0 & 0 \\ 1 & -2 & 1 & 0 \\ 0 & 1 & -2 & 1 \\ 0 & 0 & 1 & (ik\Delta x - 1) \end{pmatrix} \begin{pmatrix} \phi_1 \\ \phi_2 \\ \phi_3 \\ \phi_4 \end{pmatrix}. \quad (5)$$

It is now evident that solving the eigenvalue problem required to find the QNMs is challenging [31] as the eigenvalue  $k^2$  also appears in the boundary condition. To avoid solving this non-linear problem, it has recently been noted by Chen et al. [32] that the analysis of QNMs can be simplified by working in terms of real wave-numbers but extending the *permittivity* into the complex plane. Writing the permittivity as a spatial variation plus a constant background  $\varepsilon(x) = \varepsilon_s(x) + \varepsilon_b$  allows us to recast the Helmholtz equation as an eigenvalue problem for the permittivity

$$-\frac{1}{k^2} \left( \frac{d^2}{dx^2} + k^2\varepsilon_s(x) \right) \phi(x) = \varepsilon_b\phi(x). \quad (6)$$

Rather than using this to find the QNMs of a system, we show that this can be used to design the complex frequencies of the QNMs.

To do this, we take a known spatially varying permittivity, such as the dielectric step or absorber stack i.e. from [10], and choose a  $k \in \mathbb{C}$  at which we would like a QNM to occur. We then numerically solve the eigenvalue problem Eq. (6) using the finite difference method Eq. (5) and standard matrix libraries, to find a complex eigen-permittivity that allows us to form a structure with  $\varepsilon(x) = \varepsilon_s(x) + \varepsilon_b$  with a pole at the chosen complex frequency.

We first apply the method to the homogeneous slab. In Fig. 2 we design the new structure to support a QNM at the frequency  $k = 1.5 - 0.05i$ . For the  $N \times N$  Laplacian matrix, there are  $N$  possible values for  $\varepsilon_b$  that will satisfy this condition. Taking the lowest absolute valued background (to minimise numerical error) permittivity  $\varepsilon_b = -4.99 - 2.32i$ , we find that the new structure now supports a QNM at our chosen  $k$  (Fig. 2(a)). The transmission, Fig. 2(b), shows a large peak at the real frequency associated with the QNM, which has values  $|t| > 1$  due to the additional gain in the system. Although the location of the pole can be manipulated solely by changing the height of the barrier, in order to manipulate the real and imaginary parts independently, control over both the real and imaginary permittivity is required. In order to move a pole closer to the real frequency axis, without changing the

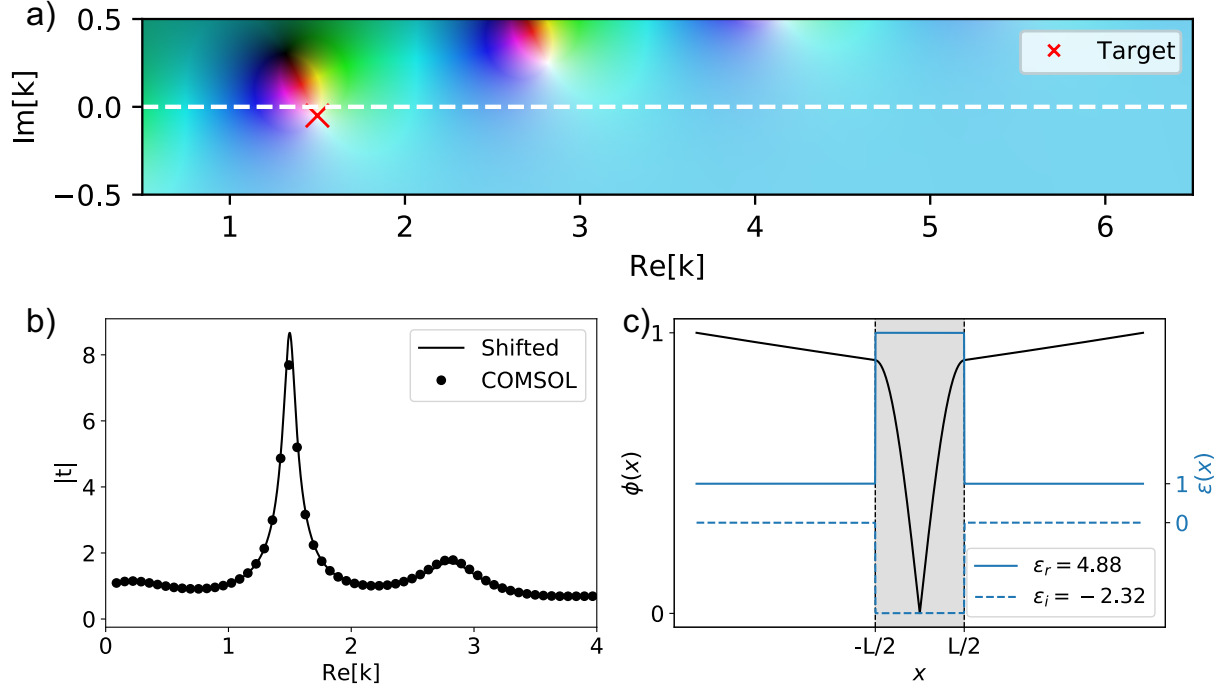


FIG. 2: A background permittivity  $\varepsilon_b = -4.99 - 2.32i$  is found as a solution to Eq. (5) which, when combined with the original structure  $\varepsilon_s(|x| < L/2) = \pi^2$  will contain a pole at the desired complex frequency of  $k = 1.5 - 0.05i$ . The reflectivity of the new structure is plotted in the complex plane (a). The transmission along the dashed white line, where  $\text{Im}[k] = 0$  is plotted (b), alongside the field distribution plotted at the complex frequency  $k$  (c). Overlaid on the transmission calculations are results found using COMSOL Multiphysics [27].

resonant frequency, gain is required. Conversely, loss is required to move the pole further away from the real axis. The field profile, shown in Fig. 2(c), still has the exponential growth characteristic of QNMs.

Next, we apply the same eigen-permittivity method to the absorbing stack shown in Fig. 1e. For this structure, we must take care that the correct boundary conditions are imposed. The opaque metal substrate requires the Dirichlet boundary condition  $\phi = 0$ , while the outgoing wave boundary condition must be imposed at the top of the stack. Choosing two target bandwidths, for the same resonance wavelength,  $\lambda_1 = (6.5 + 0.03i)\mu\text{m}$  and  $\lambda_2 = (6.5 + 0.15i)\mu\text{m}$ , we obtain background permittivities of  $\varepsilon_{b,1} = 3.27 - 0.01i$  and  $\varepsilon_{b,2} = 3.28 + 0.29i$ . The effect of the background shift on the pole locations is shown in

Fig. 3(a-b). Accordingly, the poles are found at the expected complex frequencies. The absorption, shown in Fig. 3(c) plotted along the white dashed line ( $\text{Im}[\lambda] = 0$ ) is also provided, with a fitted Lorentzian to extract the properties of the transmission resonances and verify that it corresponds to the QNMs.

Although simple to implement, this eigen-permittivity method only allows you to choose the complex frequency of a single QNM. We now explore the possibility of applying an iterative method to move one or more QNMs to desired complex frequencies, by changing the spatial variation of the permittivity profile.

### III. OPTIMISATION APPROACH TO MOVING POLES

The second method we present to move quasi-normal modes (QNMs) to desired complex frequencies is to use an iterative procedure, based on perturbation theory. Standard Rayleigh-Schrödinger perturbation theory [33] of Hermitian quantum mechanics connects a change in the potential  $\delta V$  to a change in the  $n^{\text{th}}$  energy level  $E_n$  through the matrix element

$$\delta E_n = \langle \phi_n | \delta V | \phi_n \rangle, \quad (7)$$

where the states are normalised so that  $\langle \phi_n | \phi_m \rangle = \delta_{nm}$ . Usually the perturbation to the potential is known and the energy level shifts are calculated (e.g. in the textbook analysis of the Stark effect [33] §76). Being able to analytically connect structure and function is the key to inverse design, allowing one to find derivatives of a quantity of interest (here, the energy) in terms of derivatives of the structure (the potential). With this observation, it is possible to use perturbation theory backwards to find how one should change the potential to get a particular energy level. This idea can be extended to move the complex frequency of a QNM of an electromagnetic resonator. Instead of a potential, we seek to design a permittivity profile  $\varepsilon(x)$  that has a QNM,  $k_n$ , at a particular complex frequency. However, as QNMs grow in space, they cannot be normalised. The expressions that connect a change in the permittivity profile to a change in the complex wave-number  $k_n$  requires some modification. Regularisation techniques have been used to develop a perturbation theory for QNMs in both quantum mechanics [34, 35] and electromagnetism [36]. Perturbation theory can be used to connect a change in the permittivity  $\delta\varepsilon(x)$  to a change in the complex frequency of

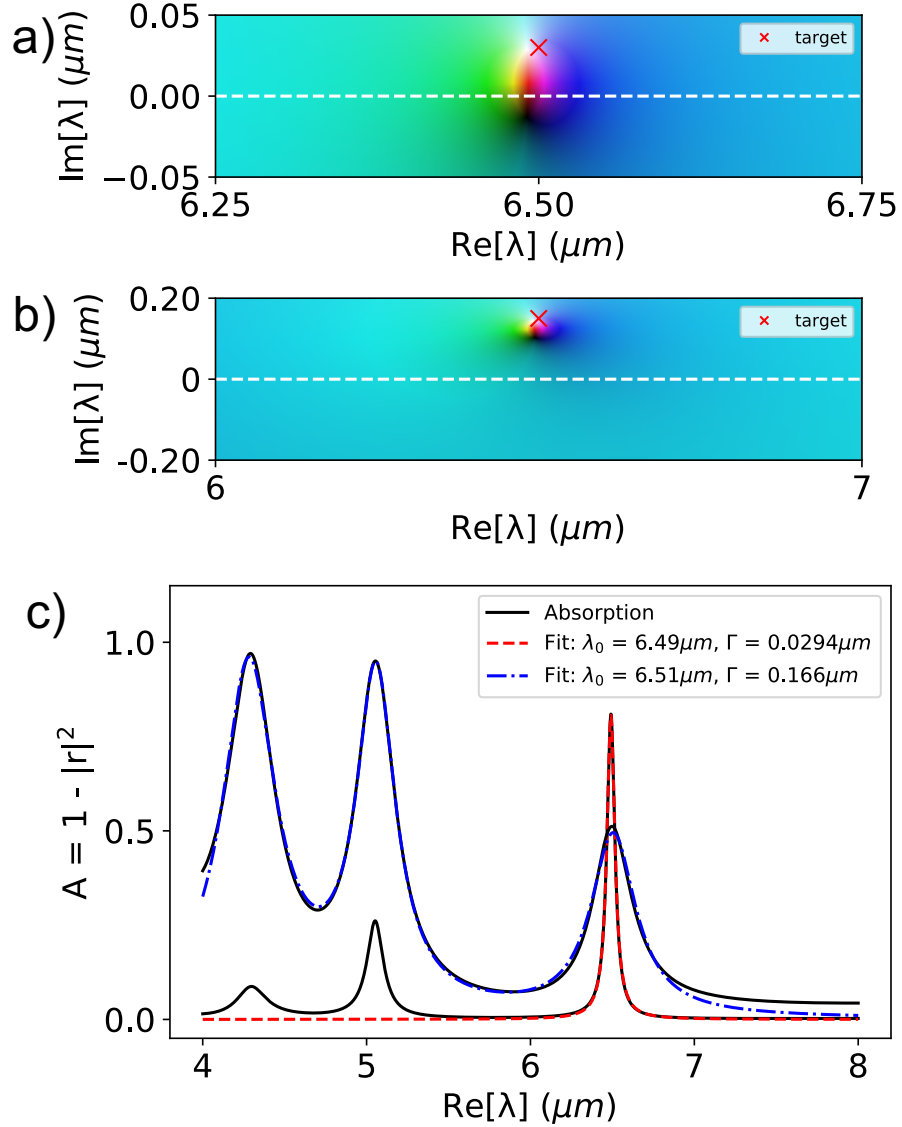


FIG. 3: The original absorbing stack, shown in Fig. 1(e) has been modified into two structures that contain a QNM at  $\lambda_1 = (6.5 + 0.03i)\mu\text{m}$  and  $\lambda_2 = (6.5 + 0.15i)\mu\text{m}$  respectively. The former is close to the real axis, corresponding to a narrow bandwidth, while the latter has a broader bandwidth. Plotted on (a) and (b) respectively are the reflection coefficients in the complex plane, showing that a QNM is indeed located at the chosen complex frequency. The absorption spectra of the two structures are plotted as a function of real wavelength (c). Fitted Lorentzians in dashed red (blue) correspond to fitting to the narrow (broad) resonance, verifying the complex frequencies of the QNMs. For the broadband case, we must fit a sum of 3 Lorentzians to accurately model the spectral profile, and obtain the correct fitting parameters.

the QNM [37] through

$$\delta k_n = \frac{1}{2k_n} \frac{\int_{-L/2}^{L/2} \phi_n^2(x) \delta \varepsilon(x) dx}{\langle \phi_n | \phi_n \rangle}, \quad (8)$$

where  $k = k' + ik''$  and the inner product is now [35]

$$\langle \phi_n | \phi_n \rangle = \int_{-L/2}^{L/2} \phi_n^2(x) dx + i [\phi_n^2(-L/2) + \phi_n^2(L/2)]. \quad (9)$$

If we change the permittivity by a small amount  $\Delta \varepsilon$  at a particular location  $x_i$  so that  $\delta \varepsilon(x) = \Delta \varepsilon \delta(x - x_i)$ , we find that

$$\delta k_n = \frac{1}{2k_n} \frac{\phi_n^2(x_i) \Delta \varepsilon}{\langle \phi_n | \phi_n \rangle}. \quad (10)$$

As this is true for all  $x_i$ , we can divide by the small change in permittivity to find the gradient of the wave-number with respect to the permittivity

$$\frac{\partial k_n}{\partial \varepsilon} = \frac{\phi_n^2(x)}{2k_n \langle \phi_n | \phi_n \rangle}. \quad (11)$$

Importantly, this gives a continuous function for the derivative of the complex frequency of the QNM with respect to the spatial structure of the permittivity. For example, say we would like to move mode  $k_n$  to the complex frequency  $k_*$ . We can write a suitable figure of merit and its derivative as

$$\mathcal{F} = (k_n - k_*)^2, \quad (12)$$

$$\frac{\partial \mathcal{F}}{\partial \varepsilon} = 2(k_n - k_*) \frac{\partial k_n}{\partial \varepsilon}. \quad (13)$$

Updating the permittivity from iteration  $i$  to  $i + 1$  is done according to

$$\varepsilon^{(i+1)}(x) = \varepsilon^{(i)}(x) + \gamma \frac{\partial \mathcal{F}}{\partial \varepsilon}, \quad (14)$$

where  $\gamma$  is the step size. This makes the evaluation of the figure of merit gradients extremely efficient, similar to the adjoint method [38]. Combining this with gradient descent optimisation [39], we have found how to update the permittivity distribution in order to arbitrarily change the complex frequencies of the QNMs.

An example of this procedure is shown in Fig. 4. We begin by selecting a QNM of the system: the frequency of which we want to modify. The complex wave-number of this mode can be found by root-finding in the complex plane, using i.e. Newton's method. Specifying a target frequency of the pole  $k_*$ , then using Eqns. (11, 13, 14) to iteratively update the

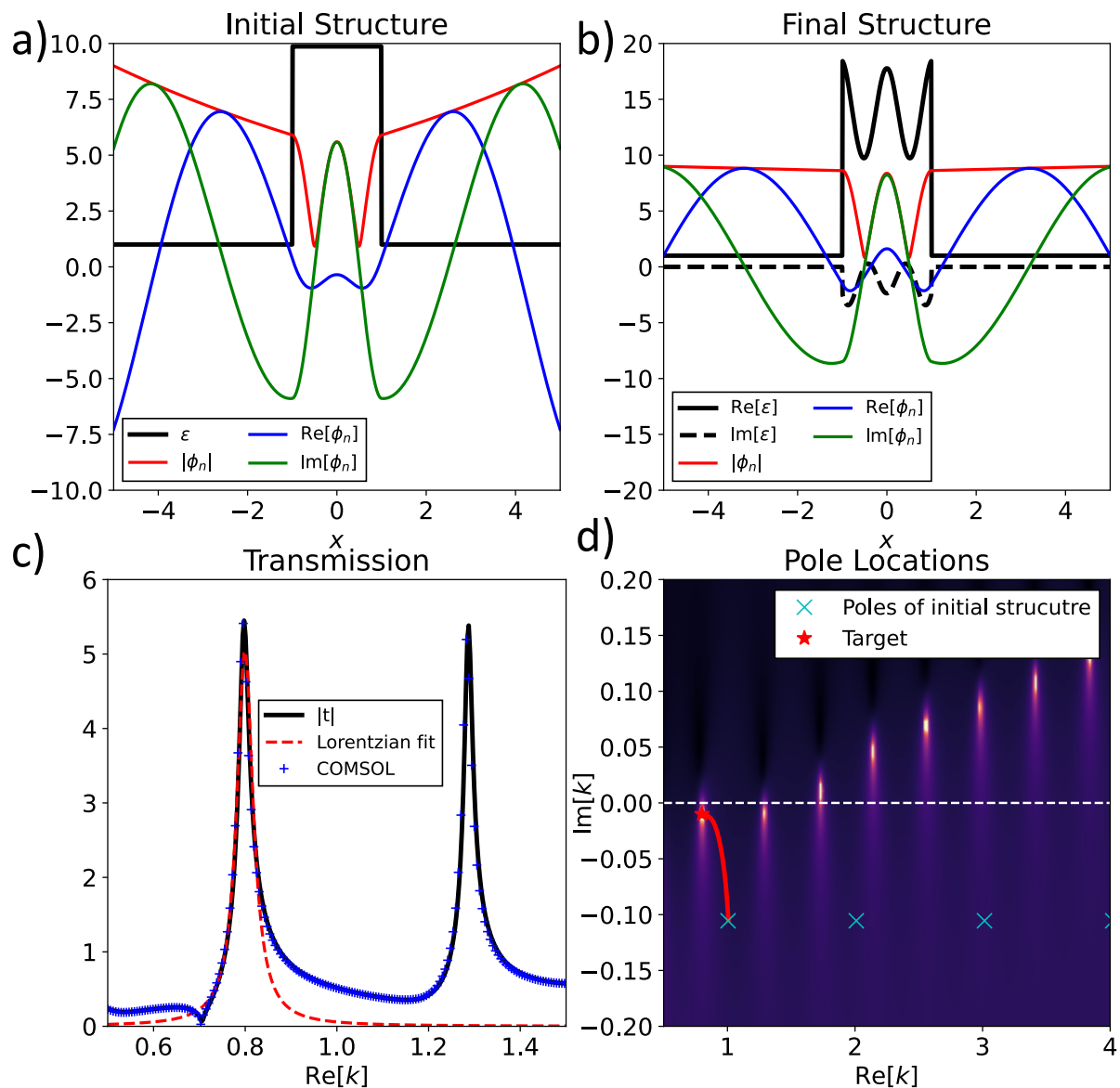


FIG. 4: An example of using our iterative method to move a pole to a desired location. Beginning from a) a step of dielectric which supports a QNM at  $k = 1 - 0.1i$ , our iterative method designs the permittivity distribution shown in b), which supports a QNM at the desired frequency  $k_* = 0.8 - 0.01i$ . The resulting transmission of the structure is shown in c), and compared to a full-wave solver. Fitting a Lorentzian to the transmission peak associated with  $k_*$ , we extract find that the peak is at  $k_0 = 0.799$  with width  $\Gamma = 0.0109$ . The path of the pole over the optimisation is shown in d).

permittivity distribution allows the pole to be moved to the desired complex frequency. At every iteration,  $\phi_n$  and  $k_n$  must be re-calculated. In the example of Fig. 4 we move the pole originally at  $k = 1 - 0.1i$  to  $k_* = 0.8 - 0.01i$ , and show that yields a structure with a peak in transmission at the designed frequency with the designed width. It should be noted that while we can move the pole to an arbitrary complex frequency, complete control of both the real and imaginary parts of the permittivity is required.

As another example of this method, we consider trying to move several poles simultaneously. In Fig. 5 we take the poles originally at  $k = 1 - 0.1i$ ,  $2 - 0.1i$  and  $3 - 0.1i$  and move them to three different values  $k_1$ ,  $k_2$  and  $k_3$ . Interestingly, due to the presence of other nearby poles, the transmission profile of the resulting structure becomes more complex, however a clear narrow transmission peaks associated with  $k_1$ ,  $k_2$  and  $k_3$  are evident. If one controls all poles of interest over a given range of  $k$  values, almost complete control over the transmission profile can be obtained.

#### IV. CONCLUSIONS AND OUTLOOK

In this work we address the inverse design problem: ‘how should one change a photonic system to ensure a quasi-normal mode appears at a pre-determined complex frequency?’. We propose two approaches to answer this question. The first is to re-express the permittivity of a system as the original permittivity profile, plus some global background shift  $\varepsilon_s(x) + \varepsilon_b$ . This allows us to write the Helmholtz equation as an eigenvalue problem for the background permittivity  $\varepsilon_b$ . By choosing a target complex frequency, we can find a (complex) background permittivity that can be added to the structure so that a QNM occurs at the desired complex frequency with the desired linewidth. This method could be used to modify existing structures to control the frequency and bandwidth of a resonant system.

The second approach we develop is an iterative procedure based on perturbation theory: a small change in permittivity can be connected to the shift in complex frequency of a QNM. By defining a suitable figure of merit, and combining with gradient descent optimisation, we can iteratively change the spatial permittivity profile to move a QNM closer to a target frequency. This procedure can also be used to move multiple QNMs to different target frequencies. This iterative approach can be further modified in many ways. For example by restricting the search space of  $\delta\varepsilon$  to only allow loss rather than gain, or to ensure  $\varepsilon(x) > 1$ .

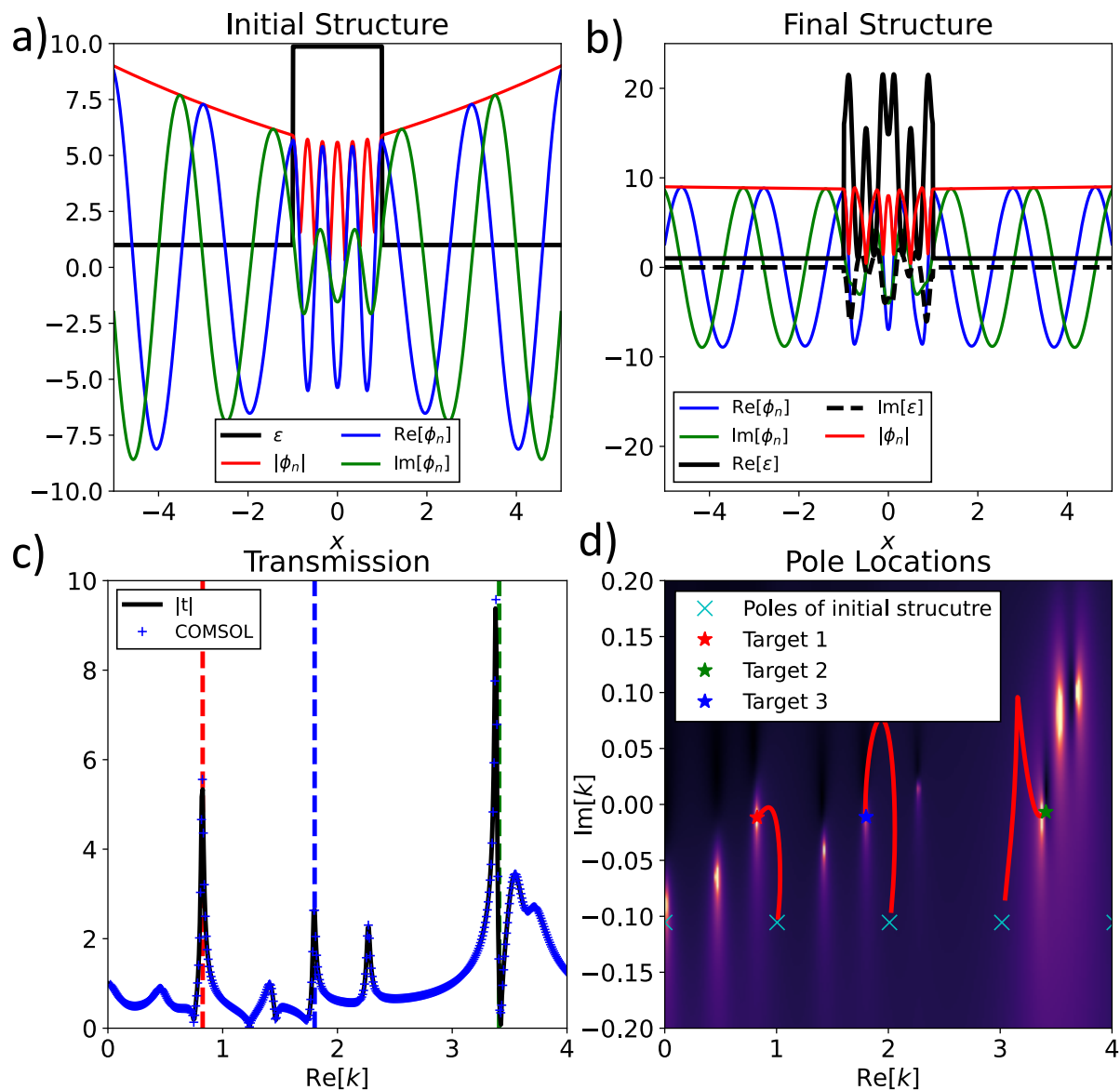


FIG. 5: An example of using the iterative method we present to move 3 poles to desired complex frequencies at the same time. Beginning from a permittivity step shown in a), the real poles associated with  $\text{Re}[k] = 1, 2, 3$  are moved to the targets:  $k_1 = 0.8 - 0.007i$ ,  $k_2 = 3.5 - 0.008i$  and  $k_3 = 1.8 - 0.009i$ . The resulting permittivity profile is shown in b) and its transmission coefficient in c). Clear peaks are seen at the three target values of  $k$ .

The path of the poles over the optimisation is shown in d).

Also, rather than manipulating the full spatial form of  $\epsilon$ , we could seek to change only a few free parameters such as width and height of the dielectric step.

The approaches we have developed open up several avenues of exploration to design, for

example, broadband absorbers for solar cells and thermal emitters. Rather than manually changing structural parameters until a QNM appears at the correct complex frequency, the methods we present leverage the benefits of inverse design to rapidly design materials that have the desired properties. Importantly, as our methods allow QNMs to be placed exactly, both resonance frequency and linewidth can be tuned with a high degree of accuracy.

## ACKNOWLEDGEMENTS

The authors would like to thank Jake Binsley for his assistance with Blender.

We acknowledge financial support from the Engineering and Physical Sciences Research Council (EPSRC) of the United Kingdom, via the EPSRC Centre for Doctoral Training in Metamaterials (Grant No. EP/L015331/1). J.R.C also wishes to acknowledge financial support from Defence Science Technology Laboratory (DSTL). S.A.R.H acknowledges financial support from the Royal Society (URF\R\211033). All data and code created during this research are openly available from the corresponding authors, upon reasonable request.

- 
- [1] G. Gamow. Zur quantentheorie des atomkernes. *Zeitschrift für Physik*, 51(204-212), 1928.
  - [2] H. A. Bethe. Nuclear physics b: Nuclear dynamics, theoretical. *Rev. Mod. Phys*, 9(69), 1937.
  - [3] S. Chandrasekhar and S. Detweiler. The quasi-normal modes of the schwarzschild black hole. *Proc. R. Soc. Lond. A*, 344(441-452), 1975.
  - [4] P. T. Kristensen, K. Herrmann, F. Intravaia, and K. Busch. Modeling electromagnetic resonators using quasinormal modes. *Adv. Opt. Photonics*, 12(612-708), 2020.
  - [5] Filippo Alpeggiani, Nikhil Parappurath, Ewold Verhagen, and L. Kuipers. Quasinormal-mode expansion of the scattering matrix. *Phs. Rev. X*, 7(021035), 2017.
  - [6] S. G. Tikhodeev, A. L. Yablonskii, E. A. Muljarov, N. A. Gippius, and T. Ishihara. Quasiguided modes and optical properties of photonic crystal slabs. *Phs. Rev. B*, 66(045102), 2002.
  - [7] Lin Zschiedrich, Felix Binkowski, Niko Nikolay, Oliver Benson, Günter Kewes, and Sven Burger. Riesz-projection-based theory of light-matter interaction in dispersive nanoresonators. *Phys. Rev. A*, 98:043806, Oct 2018.
  - [8] J. Yang, H. Giessen, and P. Lalanne. Simple analytical expression for the peak-frequency

- shifts of plasmonic resonances for sensing. *Nano Lett.*, 15(3439-3444), 2015.
- [9] S. Both, M. Schäferling, F. Sterl, E. A. Muljarov, H. Giessen, and T. Weiss. Nanophotonic chiral sensing: How does it actually work? *ACS Nano.*, 16(2822-2832), 2022.
- [10] A Sakurai, K Yada, T Simomura, S Ju, M Kashiwagi, H Okada, T Nagao, K Tsuda, and J Shiomi. Ultranarrow-Band Wavelength-Selective Thermal Emission with Aperiodic Multi-layered Metamaterials Designed by Bayesian Optimization. *ACS Cent. Sci.*, 5(2):319–326, feb 2019.
- [11] M. De Zoysa, T. Asano, K. Mochizuki, A. Oskooi, T. Inoue, and Susumu Noda. Conversion of broadband to narrowband thermal emission through energy recycling. *Nature Photon.*, 6(535-539), 2021.
- [12] N. Liu, M. Mesch, T. Weiss, M. Hentschel, and H. Giessen. Infrared perfect absorber and its application as plasmonic sensor. *Nano. Lett.*, 10(2342-2348), 2010.
- [13] N. I. Landy, S. Sajuyigbe, J. J. Mock, D. R. Smith, and W. J. Padilla<sup>1</sup>. Perfect metamaterial absorber. *Phys. Rev. Lett.*, 100(207402), 2008.
- [14] S. Luo, J. Zhao, D. Zuo, and X. Wang. Perfect narrow band absorber for sensing applications. *Opt. Express*, 24(9288-9294), 2016.
- [15] A. Lochbaum, Y. Fedoryshyn, A. Dorodnyy, U. Koch, C. Hafner, and J. Leuthold. On-chip narrowband thermal emitter for mid-ir optical gas sensing. *ACS Photonics*, 4(1371-1380), 2017.
- [16] K. Aydin, V. E. Ferry, R. M. Briggs, and H. A. Atwater. Broadband polarization-independent resonant light absorption using ultrathin plasmonic super absorbers. *Nat. Commun.*, 2(517), 2011.
- [17] R. A. Pala, J. White, E. Barnard, J. Liu, and M. L. Brongersma. Design of plasmonic thin-film solar cells with broadband absorption enhancements. *Adv. Mater.*, 21(3504-3509), 2009.
- [18] Y. Zhou, Z. Qin, Z. Liang, D. Meng, H. Xu, D. R. Smith, and Y. Liu. Ultra-broadband metamaterial absorbers from long to very long infrared regime. *Light Sci Appl*, 10(138), 2021.
- [19] F. Ding, J. Dai, Y. Chen, J. Zhu, Y. Jin, and S. I. Bozhevolnyi. Broadband near-infrared metamaterial absorbers utilizing highly lossy metals. *Scientific Reports*, 6(39445), 2016.
- [20] S. Molesky, Z. Lin, A. Y. Piggott, W. Jin, J. Vucković, and A. W. Rodriguez. Inverse design in nanophotonics. *Nature Photon.*, 12(659–670), 2018.
- [21] V. Grigoriev, A. Tahri, S. Varault, B. Rolly, B. Stout, J. Wenger, and N. Bonod. Optimization

- of resonant effects in nanostructures via weierstrass factorization. *Phys. Rev. A*, 88(011803), 2013.
- [22] T. Wu, A. Baron, P. Lalanne, and K. Vynck. Intrinsic multipolar contents of nanoresonators for tailored scattering. *Phys. Rev. A*, 101(011803), 2020.
- [23] X. Ming and L. Sun. Optimization of broadband perfect absorber by weierstrass factorization. *IEEE Photonics J.*, 11(IEEE Photonics J.), 2019.
- [24] Wei Yan, Philippe Lalanne, and Min Qiu. Shape deformation of nanoresonator: A quasinormal-mode perturbation theory. *Phys. Rev. Lett.*, 125:013901, Jul 2020.
- [25] P. Virtanen et al. SciPy 1.0: fundamental algorithms for scientific computing in Python. *Nat. Methods*, 17(3):261–272, 2020.
- [26] M Born and E Wolf. *Principles of Optics*. Elsevier, 2013.
- [27] COMSOL Multiphysics v. 6.0, 2022.
- [28] A. Sommerfeld. *Partial Differential Equations in Physics*. Academic Press, 1949.
- [29] F. J. Zerilli. Effective potential for even-parity regge-wheeler gravitational perturbation equations. *Phys. Rev. Lett.*, 24(737-738), 1970.
- [30] P. L. Kapur and R. Peierls. The dispersion formula for nuclear reactions. *Proc. R. Soc. Lond. A*, 166(277-295), 1938.
- [31] P. Lalanne, W. Yan, A. Gras, C. Sauvan, J.-P. Hugonin, M. Besbes, G. Demésy, M. D. Truong, B. Gralak, F. Zolla, A. Nicolet, F. Binkowski, L. Zschiedrich, S. Burger, J. Zimmerling, R. Remis, P. Urbach, H. T. Liu, and T. Weiss. Quasinormal mode solvers for resonators with dispersive materials. *J. Opt. Soc. Am. A*, 36(686-704), 2019.
- [32] P. Y. Chen, D. J. Bergman, and Y. Sivan. Generalizing normal mode expansion of electromagnetic green’s tensor to open systems. *Phys. Rev. Appl.*, 11(044018), 2019.
- [33] L. D. Landau and E. M. Lifshitz. *Quantum Mechanics: Non-relativistic Theory*. Pergamon Press, 2rd edition, 1965.
- [34] Y. B. Zel’Dovich. On the theory of unstable states. *Soviet Physics JETP*, 12(3), 1961.
- [35] P. T. Leung, Y. T. Liu, W. M. Suen, C. Y. Tam, and K. Young. Logarithmic perturbation theory for quasinormal modes. *J. Phys. A*, 31(3271), 1998.
- [36] E. A. Muljarov, W. Langbein, and R. Zimmermann. Brillouin-wigner perturbation theory in open electromagnetic systems. *EPL*, 92(50010), 2010.
- [37] A. M. Perelomov and Y. B. Zel’Dovich. *Quantum Mechanics: Selected Topics*. World Scientific,

1998.

- [38] C. M. Lalau-Keraly, S. Bhargava, O. D. Miller, and E. Yablonovitch. Adjoint shape optimization applied to electromagnetic design. *Opt. Express*, 21:21693–21701, 2013.
- [39] W. H. Press, S. A. Teukolsky, W. T. Vetterling, and B. P. Flannery. *Numerical Recipes: The Art of Scientific Computing (3rd Ed.)*. Cambridge University Press, 2007.